Bypassing the filtering challenges in microwave-optical quantum transduction through optomechanical four-wave mixing

James Schneeloch,* Erin Sheridan, A. Matthew Smith, Christopher C. Tison, Daniel L. Campbell, Matthew D. LaHaye, Michael L. Fanto, and Paul M. Alsing
Air Force Research Laboratory, Information Directorate, Rome, New York 13441, USA

(Received 6 December 2024; revised 3 April 2025; accepted 3 June 2025; published 2 July 2025)

Microwave-optical quantum transduction is a key enabling technology in quantum networking, but has been plagued by a formidable technical challenge. As most microwave-optical-transduction techniques rely on three-wave mixing processes, the processes consume photons from a driving telecom-band (pump) laser to convert input microwave photons into telecom-band photons detuned from the laser by this microwave frequency. However, cleanly separating out single photons detuned only a few GHz away from a classically bright laser in the same spatial mode requires frequency filters of unprecedented extinction over a very narrow transition band, straining the capabilities of today's technology. Instead of confronting this challenge directly, we show how one may achieve the same transduction objective with comparable efficiency using a four-wave mixing process in which *pairs* of pump photons are consumed to produce transduced optical photons widely separated in frequency from the pump. We develop this process by considering higher-order analogues of photoelasticity and electrostriction than those used in conventional optomechanics, and examine how the efficiency of this process can be made to exceed conventional optomechanical couplings.

DOI: 10.1103/f35f-4128

I. INTRODUCTION

Quantum transduction between light and sound (converting between acoustic phonons and photons) is a critical intermediate process employed in the more promising technologies toward making large-scale quantum networking possible [1–4]. Of particular relevance to the subject of this paper, piezo-optomechanical transduction [5–9] uses a piezoelectric interaction to convert microwave photons from superconducting-circuit (SC) qubits into acoustic phonons of the same frequency, and then an optomechanical interaction to convert these sound quanta into telecom-band photons by consuming pump photons from a laser to make up the energy difference.

As a three-wave mixing process between two photons and one phonon, the optomechanical interaction these transducers employ introduces a formidable technical challenge in filtering. The difference in frequency between the transduction photons and the pump photons is about five orders of magnitude smaller than either one itself (e.g., a detuning of 2 GHz from a central frequency of 200 THz). Moreover, one must filter the pump aggressively enough that both no fringe pump photons are in the transduction band, and that the transduction band photons can be picked out without picking up residual pump photons. Accomplishing this directly requires developing filtering technology of unprecedented extinction for so narrow a transition band. Though highly dispersive filters exist that may cleanly separate spectral lines with similar detunings [10–12], and there are proposed schemes of concatenating multiple filters to achieve high extinction [13], the simultaneous challenge of achieving the high extinction ratios needed for *single-photon* quantum transduction is as yet unmet.

That said, the related photon-phonon pair generation process (what we will call optomechanical down-conversion) occurring when the transducers are driven with a blue-detuned pump (where annihilated pump photons of energy higher than the transduction-band are down-converted into photon-phonon pairs) does not suffer from such stringent filtering requirements [14–17]. In optomechanical down-conversion, one may use short pump pulses of high peak power to create these photon-phonon pairs with reduced overall pump *energy*. For the relatively small number of pump photons needed to facilitate this optomechanical down-conversion, the pump can be filtered effectively from the transduced photons with state-of-the-art optics. Unfortunately, these techniques that dramatically increase the efficiency of optomechanical down-conversion cannot be used to also enhance the efficiency of quantum transduction (occurring when the system is operated with a red-detuned pump) because high-fidelity quantum transduction requires a driving pump whose bandwidth is much narrower than that of the input photons, precluding utilizing short pump pulses.

In this work, we show how to circumvent this filtering challenge of single-photon quantum transduction using a novel *four*-wave mixing process between three photons and one

*Contact author: james.schneeloch.1@afrl.af.mil

Published by the American Physical Society under the terms of the Creative Commons Attribution 4.0 International license. Further distribution of this work must maintain attribution to the author(s) and the published article's title, journal citation, and DOI.

acoustic phonon. Importantly, we will illustrate how this new mechanism allows one to obtain comparable optomechanical couplings to existing quantum transducers, demonstrating that comparable transduction efficiencies can be achieved.

The coupling between sound (i.e., strain) in a material and the electromagnetic energy passing through it has been studied in one form or another for more than 140 years [18–21]. Regarding the first (linear) order in the mechanical and electric displacement fields, we have the forward and converse piezoelectric effects. For the second order, we have electrostriction and photoelasticity, and it is at this order that we have the standard three-wave-mixing optomechanical interaction. At each order, these properties are connected thermodynamically by Maxwell relations, or generalizations thereof.

Extrapolating to the *third*-order relationship between the mechanical and electric displacement fields, one may show (as is worked out in Appendix A) that what we call the second-order photoelasticity (i.e., the rate of change in second-order nonlinear inverse permittivity with respect to applied strain) is thermodynamically connected to a *cubic* electrostriction (induced strain proportional to the cube of the applied electric field). Far from being an esoteric relation between physically insignificant factors, we demonstrate how this third-order connection can amount to a substantial optomechanical coupling without suffering from the same filtering challenges as in the standard case.

Although higher-order photon-phonon interactions were first examined over fifty years ago [20], the field remains largely unexplored, with the exception of using a second-order photoelasticity to examine stress-induced changes to second-order optical nonlinearity [22] and in AMO-based ensembles [23–26]. To our knowledge, our work herein represents the first study of this higher-order interaction in an optomechanical platform for quantum transduction.

In this work, we demonstrate the feasibility of microwave—telecom quantum transduction using optomechanical four-wave mixing. While the standard optomechanical three-wave mixing process consumes individual pump photons to facilitate transduction, optomechanical four-wave mixing consumes *pairs* of pump photons to facilitate transduction, as illustrated in the energy level diagrams in Fig. 1. Where the transduction photons in this case have nearly twice the frequency of any one pump photon, both pump and transduced light can be easily filtered to high extinction with conventional optical filters.

The total efficiency of the quantum transduction process (as given by the square of the amplitude to produce a photon in the transduced optical mode, given an initial photon in the input microwave mode) depends on many factors relating to the coupling between different modes in the transduction process, as well as the relations between each coupling. For a more thorough explanation, we recommend the references [5] and [27]. To facilitate a side-by side comparison between an ordinary transducer utilizing optomechanical three-wave mixing, and our proposed mechanism employing optomechanical four-wave mixing, we shall consider both processes as comparably efficient when (all other factors constant) the effective optomechanical coupling is the same in both cases.

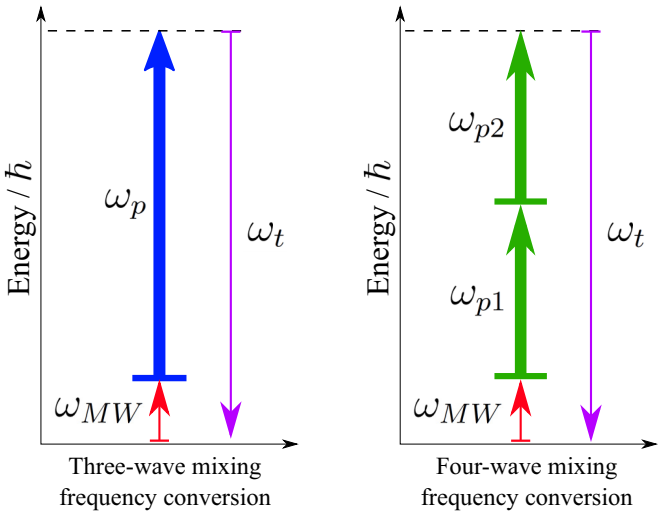


FIG. 1. Energy-level diagram showing the difference between three- and four-wave mixing processes in frequency conversion from a GHz phonon at $\omega = \omega_{MW}$ to a telecom-band photon at $\omega = \omega_t$. The arrows in bold are classically bright fields at frequencies ω_p, ω_{p1}, and ω_{p2}, respectively, which provide the required energy for the conversion to occur.

Though we discuss the full optomechanical coupling for both a three-wave and four-wave mixing interaction in Appendix B, we point out that the optomechanical coupling for both interactions can be regarded as proportional to an effective photoelasticity. For the standard three-wave mixing-based coupling, we may use the photoelasticity as tabulated in tables of material parameters to gauge the strength of the effective coupling. For the case of our novel four-wave mixing, we may combine the second-order photoelasticity (defined presently) with one factor of the electric displacement field to obtain a comparable factor we call a *virtual photoelasticity*. To facilitate this side-by-side comparison, we also develop a formula for the second-order photoelasticity using standard material parameters.

II. OPTOMECHANICAL INTERACTIONS

A. Standard case: First-order photoelasticity

The optomechanical interaction in microwave-optical quantum transduction can be expressed by considering how the strain tensor x_{ij} in a material alters its inverse permittivity η_{ij}. To first order, we can describe this as

$$\epsilon_0 \eta_{ij(\mathrm{eff})}(x_{k\ell}) \approx \epsilon_0 \eta_{ij}(0) + p_{ijk\ell(\mathrm{eff})} x_{k\ell}, \tag{1}$$

where the effective photoelasticity tensor $p_{ijk\ell(\mathrm{eff})}$ is defined as [28] the derivative of the *relative* inverse permittivity $\epsilon_0 \eta_{ij}$ with respect to strain $x_{k\ell}$ for small strain;

$$p_{ijk\ell(\mathrm{eff})} \equiv \epsilon_0 \left(\frac{\partial \eta_{ij(\mathrm{eff})}}{\partial x_{k\ell}} \bigg|_{x \to 0} \right). \tag{2}$$

Note that the effective photoelasticity incorporates the true bulk photoelasticity of the material, as well as other contributions due to shifting boundaries, among other effects. Also, we will use the Einstein summation convention in this work for repeated indices (unless otherwise stated) to simplify notation.

As part of the total Hamiltonian for the electromagnetic field of a linear dielectric [29], i.e.,

$$\hat{H} = \frac{1}{2}\int d^3r\left(\eta_{ij}^{(1)}\hat{D}_i\hat{D}_j + \frac{1}{\mu_{ij}}\hat{B}_i\hat{B}_j\right), \tag{3}$$

where the hats denote quantum operators, the strain-induced shift to $\eta_{ij}^{(1)}$ yields an additional term we call the optomechanical interaction Hamiltonian,

$$\hat{H}_{\text{int}}^{(1)} = \frac{1}{2\epsilon_0}\int d^3r\left(p_{ijk\ell(\text{eff})}\hat{D}_i\hat{D}_j\hat{x}_{k\ell}\right), \tag{4}$$

which is second-order in the electric displacement field $\hat{D}$, and first-order in the mechanical (acoustic) displacement u_i, by virtue of the strain x_{ij} being given by the gradient of the displacement: $\frac{\partial\hat{u}_i}{\partial r_j}$, in the absence of rotational motion.

This interaction Hamiltonian $\hat{H}_{\text{int}}^{(1)}$ yields the simple optomechanical interaction Hamiltonian after linearizing it on the assumption of a classically bright pump. Overall, the form of the optomechanical interaction (in the single-mode approximation) can be expressed simply in terms of an optomechanical coupling constant G_{OM}:

$$\hat{H}_{\text{int}}^{(1)} = \hbar G_{OM}(\hat{a}+\hat{a}^\dagger)(\hat{b}+\hat{b}^\dagger), \tag{5}$$

where G_{OM} includes factors proportional to the pump amplitude, the photoelasticity, and the overlap integral that covers the spatial variation of the field modes. For a more extensive discussion of this, see [27].

B. Second-order photoelasticity and optomechanical four-wave mixing

Between a vanishing electric field and an electric field so large that it ionizes the solid, the inverse permittivity η_{ij} is more generally a nonlinear function of D_k that can be represented by the following power series:

$$\eta_{ij} = \eta_{ij}^{(1)} + \eta_{ijk}^{(2)}D_k + \eta_{ijk\ell}^{(3)}D_kD_\ell + \ldots, \tag{6}$$

where, for example, the second-order inverse optical susceptibility is given by

$$\eta_{hij}^{(2)} \equiv \left(\frac{\partial\eta_{hi}}{\partial D_j}\bigg|_{D\to 0}\right. . \tag{7}$$

Just as the ordinary photoelasticity $p_{ijk\ell}$ describes the first-order change to $\eta_{ij}^{(1)}$ with respect to strain $x_{k\ell}$, we define the second-order photoelasticity $q_{hijk\ell}$ to be the second-order change to the relative permittivity $(\epsilon_0\eta_{hi})$ with respect to electric displacement field D_k and strain $x_{k\ell}$;

$$q_{hijk\ell} \equiv \epsilon_0\left(\frac{\partial^2\eta_{hi}}{\partial x_{k\ell}\partial D_j}\bigg|_{(D,x)\to 0} = \epsilon_0\left(\frac{\partial\eta_{hij}^{(2)}}{\partial x_{k\ell}}\bigg|_{x\to 0}\right. . \tag{8}$$

Note that while the ordinary photoelasticity $p_{ijk\ell}$ is dimensionless, the second-order photoelasticity $q_{ijk\ell m}$ has dimensions of m^2/C.

Following from Eqs. (4) and (6), the electromagnetic Hamiltonian for a second-order *nonlinear* dielectric [29,30] is given by [31]

$$\hat{H} = \frac{1}{2}\int d^3r\left(\eta_{ij}^{(1)}\hat{D}_i\hat{D}_j + \frac{1}{\mu_{ij}}\hat{B}_i\hat{B}_j\right) + \frac{1}{3}\int d^3r\left(\eta_{ijk}^{(2)}\hat{D}_i\hat{D}_j\hat{D}_k\right). \tag{9}$$

If we include the effect of both first- and second-order photoelasticity, we obtain an additional higher-order optomechanical interaction term given by

$$\hat{H}_{\text{int}}^{(2)} = \frac{1}{3\epsilon_0}\int d^3r\left(q_{hijk\ell}\hat{D}_h\hat{D}_i\hat{D}_j\hat{x}_{k\ell}\right), \tag{10}$$

which is third-order in the electromagnetic field and first-order in the mechanical displacement field, making it a four-wave mixing interaction Hamiltonian.

Under the assumption of a bright pump, this four-wave mixing interaction Hamiltonian can also be approximated as a linearized optomechanical interaction Hamiltonian of the same form as the first-order photoelastic interaction. The primary differences are that the optomechanical coupling G_{OM} will: (i) be proportional to pump power rather than pump amplitude; (ii) be proportional to second-order photoelasticity $q_{hijk\ell}$; and (iii) depend on the overlap integral of four modes (three optical, one acoustic) instead of three. See Appendix B for discussion.

1. *Estimating second-order photoelasticity*

In order to understand the significance of this optomechanical four-wave mixing interaction, we must be able to estimate the value of $q_{hijk\ell}$ for different materials and perform a side-by-side comparison of this with the standard three-wave mixing interaction from Eq. (4). To estimate the value of the second-order photoelasticity $q_{hijk\ell}$, we make use of Miller's rule in nonlinear optics [32,33], which approximates the second-order nonlinear susceptibility at the three frequencies being mixed as proportional to the product of the first-order susceptibilities at each respective frequency. In terms of inverse optical susceptibilities, Miller's rule takes the following form:

$$\eta_{hij}^{(2)}(\omega_3=\omega_1+\omega_2) = -Q\prod_{s=1,2,3}\left(1-\epsilon_0\eta_{ss}^{(1)}(\omega_s)\right), \tag{11}$$

where Q is a constant of proportionality (independent of frequency). If we assume the constant of proportionality Q is a constant for each material, and that we are in a coordinate frame that diagonalizes $\eta_{ij}^{(1)}$, then we may obtain the approximate empirical formula for the second-order photoelasticity without needing to know the value of Q;

$$q_{hijk\ell} = \epsilon_0\frac{\partial\eta_{hij}^{(2)}}{\partial x_{k\ell}} \approx -\epsilon_0\eta_{hij}^{(2)}\sum_{s=1,2,3}\frac{p_{sskl}(\omega_s)}{1-\epsilon_0\eta_{ss}^{(1)}(\omega_s)}. \tag{12}$$

This is accomplished by differentiating our expression for $\eta_{hij}^{(2)}$ [Eq. (11)] with respect to strain, and eliminating Q in the resulting expression by substituting its value, as determined by Eq. (11). In terms of conventionally tabulated parameters, our expression for the second-order photoelasticity may be simplified and approximated to

$$q_{(\text{eff})k\ell} \approx -\frac{2d_{\text{eff}}}{\epsilon_0 n^2(\omega_1)n^2(\omega_2)n^2(\omega_3)}\sum_{s=1,2,3}\frac{p_{sskl}(\omega_s)}{1-\frac{1}{n^2(\omega_s)}}, \tag{13}$$

where the indices of refraction at the given frequencies are taken along the appropriate polarizations, and d_{eff} is half the effective value of the second-order nonlinear optical susceptibility $\chi_{\text{eff}}^{(2)}$, accounting for quasi-phase-matching factors as necessary [34]. Note that we use d_{eff} instead of the inverse nonlinear-optical susceptibility because the latter is not

commonly tabulated, which is made possible through the conversion formula [29]:

$$\eta^{(2)}_{ijk} = -\epsilon_0 \eta^{(1)}_{i\ell} \chi^{(2)}_{\ell mn} \eta^{(1)}_{mj} \eta^{(1)}_{nk} \tag{14a}$$

$$\eta^{(2)}_{\text{eff}} \approx -\frac{\chi^{(2)}_{\text{eff}}}{\epsilon_0^2 n_p^2 n_1^2 n_2^2} = -\frac{2d_{\text{eff}}}{\epsilon_0^2 n_p^2 n_1^2 n_2^2}. \tag{14b}$$

For the transduction process under consideration, we let $(\omega_1 = \omega_{p1}, \omega_2 = \omega_{p2}, \omega_3 = \omega_t = \omega_{p1} + \omega_{p2} + \omega_m)$.

With our formula for q_{eff} (13), we can enter constants to see what a typical value for q_{eff} might be. As an example, for Barium titanate (selected for its large nonlinearity and photoelasticity), where $n(2\pi c/1310\,\text{nm}) \approx 2.27$, $n(2\pi c/2600\,\text{nm}) \approx 2.26$ [35], $d_{\text{eff}} \approx 10$ pm/V [36–38], $p_{1133} \approx 0.2^{**}$, $p_{2233} \approx 0.2^{**}$, $p_{3333} \approx 0.77^{**}$ [39,40], this gives an effective second-order photoelasticity $q^{(\text{eff})} \approx 2.45 \times 10^{-2}\,\text{m}^2/\text{C}$. Alternative materials with higher d_{eff} and lower photoelasticity by approximately the same fraction will have comparable values of second-order photoelasticity—such as periodically poled Lithium niobate, which, with material parameters given in [41–43], implies an approximate value for $q^{(\text{eff})}$ of $3.22 \times 10^{-2}\,\text{m}^2/\text{C}$. That said, materials with no second-order nonlinearity due to a centrosymmetric structure will also have no second-order photoelasticity.

Because the second-order photoelasticity $q_{hijk\ell}$ is an odd-rank tensor, it must be identically zero for centrosymmetric media. This may appear to conflict with experimental evidence of strain-induced second-order nonlinearity in silicon [44], a centrosymmetric medium. However, a strain-*gradient*-induced second-order nonlinearity exists in silicon because a spatially varying strain breaks this centrosymmetry [45]. Indeed, one can tabulate this effect in terms of an even-rank tensor where the inverse nonlinear susceptibility $\eta^{(2)}_{hij}$ is differentiated with respect to the strain gradient $\frac{\partial x_{k\ell}}{\partial r_m}$, but this is beyond the scope of this work. That said, for the large frozen-in strain gradients that can exist at the interface between Silicon and Silicon nitride, this is a promising means to realize second-order nonlinear processes in silicon photonics [45,46].

In what follows, we will show how the optomechanical coupling using second-order photoelasticity compares with conventional approaches.

2. Comparison of relative interaction strengths

Where the optomechanical three-wave-mixing (4) and four-wave-mixing interaction Hamiltonians (10) differ by only a few factors, we may group $q_{hijk\ell}$ with $\hat{D}_h$ and other constant factors to emulate a (virtual) first-order photoelasticity $p^{(\text{virt})}_{ijk\ell}$:

$$\hat{H}^{(2)}_{\text{int}} = \frac{1}{2\epsilon_0} \int d^3r \left(p^{(\text{virt})}_{ijk\ell} \hat{D}_i \hat{D}_j \hat{x}_{k\ell} \right), \tag{15}$$

where

$$p^{(\text{virt})}_{ijk\ell} = 2q^{(\text{eff})}_{hijk\ell} \hat{D}_h = 2\epsilon_0 q^{(\text{eff})}_{hijk\ell} (\epsilon_R)_{hm} \hat{E}_m. \tag{16}$$

For our example with barium titanate, we had a $q^{(\text{eff})} \approx 2.45 \times 10^{-2}\,\text{m}^2/\text{C}$, and $\epsilon_R \approx 5.09$. In these units, $p^{(\text{virt})}_{ij\ell m} \approx 2.21 \times 10^{-12} \hat{E}_i$. Where the average electric field of a Gaussian beam of light propagating through a barium titanate waveguide with mode field diameter (MFD) of 1.2 μm [47] has an average peak electric field amplitude given by the following relation:

$$|E| \approx \sqrt{\frac{16P}{n\pi\epsilon_0 c\,(\text{MFD})^2}}, \tag{17}$$

which—within an order of magnitude at 1 mW power—would be approximately $7.68 \times 10^5\,\text{V/m}$, corresponding to a peak intensity of $88.4\,\text{kW/cm}^2$, well below its optical damage threshold of $0.54\,\text{GW/cm}^2$ [48] (about 6.11 W for this beam diameter), [49]. As a general function of power P, these parameters give a virtual photoelasticity $p^{(\text{virt})}$ of about $5.36 \times 10^{-5}\sqrt{P}$. While this is rather small compared to the nominal photoelasticity of 0.77 for barium titanate, it may still be sufficient for efficient quantum transduction to occur.

III. DISCUSSION OPTIMIZING OPTOMECHANICAL FOUR-WAVE MIXING

For the proposed transducer in [5], as demonstrated in [9], the single-photon optomechanical coupling g_0 is about $2\pi \times 400\,\text{Hz}$, where other optomechanical transducers may have couplings as high as $2\pi \times 850\,\text{kHz}$ [50], with the majority of this increase coming from design, rather than different bulk material properties. All other material parameters constant, and using the parameters of the transducer in [5] as a benchmark, then the rapid growth of the overall optomechanical coupling in optomechanical four-wave mixing relative to the standard approach shows that optimal transduction may be achieved with powers of the order $10^1\,\text{W}$. While this is currently above the damage threshold of Barium titanate, any further enhancements to the cumulative factor of nonlinearity and photoelasticity ($d_{\text{eff}}\, p_{ssk\ell}$) (e.g., by electrically polarizing the medium with a DC electric field [51]), may enable near-unity transduction efficiencies at intensities below the optical damage threshold of the material. Indeed, the same improvements, which lower the required pump power for high transduction efficiency, will also mitigate effects of heating the transducer, which would otherwise be a problematic source of noise generated from an increased population of thermal microwave photons being transduced, in addition to the intended signal.

Independent of bulk material properties, the propensity for optomechanical four-wave mixing is effected by the magnitude of the overlap Φ of all four field modes in the region of interaction:

$$\Phi = \int d^3r \mathcal{E}_{(p1)}(\vec{r}) \mathcal{E}_{(p2)}(\vec{r}) \mathcal{E}^*_{(tr)}(\vec{r}) x_{MW}(\vec{r}) \Gamma(\vec{r}), \tag{18}$$

where $\mathcal{E}_{(p1)}$ and $\mathcal{E}_{(p2)}$ are the field eigenmodes for the first and second pump photon; $\mathcal{E}_{(tr)}$ is the field eigenmode for the transduction-band photon, $x_{MW}(\vec{r})$ is the field eigenmode for the acoustic phonon, and $\Gamma(\vec{r})$ is a bounding function describing the region of interaction (i.e., is unity inside the region and zero outside the region). When the eigenmodes are fully confined by the medium, $\Gamma(\vec{r})$ may be neglected and replaced by unity. (See Appendix B for derivation of overlap integral.)

The overlap integral from Eq. (18) is often broken up (for beamlike modes) as the product of a transverse-overlap integral (describing transverse spatial mode matching) and a longitudinal overlap integral describing the phase-matching conditions similar to those seen in nonlinear optics. In general, tighter mode confinement will improve the transverse

overlap, which motivates using high-index waveguides. The longitudinal overlap (assuming an approximately rectangular geometry with a periodic poling of period Λ to compensate for any momentum offset) is proportional to the phase-matching integral

$$\Phi \propto \left(\int dz e^{i\Delta k_z z} \right), \tag{19}$$

where z ranges from zero to L, the length of the medium, and

$$\Delta k_z = k_{tz} - k_{p1z} - k_{p2z} - k_{MWz} - k_{\Lambda z}. \tag{20}$$

For co-propagating transduction, where the input photons and phonon are propagating in the same direction, all momenta in Eq. (20) have the same sign and we get:

$$\Delta k_z^{(\text{co-prop})} \approx \frac{n(\omega_t)\omega_t}{c} - \frac{n(\omega_{p1})\omega_{p1}}{c} - \frac{n(\omega_{p2})\omega_{t2}}{c} - \frac{\omega_{MW}}{v_{sMW}} - \frac{2\pi}{\Lambda}, \tag{21}$$

where v_{sMW} is the speed of sound in the material for this acoustic mode. Alternatively, one may consider counter-propagating transduction, where the two pump photons have equal and opposite momenta, canceling each other out, leading to the following condition:

$$\Delta k_z^{(\text{counter-prop})} \approx \frac{n(\omega_t)\omega_t}{c} - \frac{\omega_{MW}}{v_{sMW}} - \frac{2\pi}{\Lambda}, \tag{22}$$

which may be an easier condition to satisfy, depending on the acoustic properties of the transduction media.

When the transducer is designed with a geometry whose eigenmodes are not beamlike, in the sense that they can be readily separated into a product of longitudinal and transverse mode functions, one can still gain intuition on optimal design arrangements. As discussed in Appendix C, one can examine the overlap integral Φ in momentum space to find that it is proportional to the momentum-conserving portion of the total integral over all momenta of the product of all interacting modes:

$$\Phi \propto \int d^3k_{p1} \int d^3k_{p2} \int d^3k_t \int d^3k_{MW} \times \tilde{\mathcal{E}}_{(p1)}(\vec{k}_{p1})\tilde{\mathcal{E}}_{(p2)}(\vec{k}_{p2})\tilde{\mathcal{E}}^*_{(tr)}(\vec{k}_t)\tilde{x}_{MW}(\vec{k}_{MW})\tilde{\Gamma}\left(\sum_q \vec{k}_q \right), \tag{23}$$

where $\tilde{x}_{MW}(\vec{k}_{MW})$ is the spatial Fourier transform of $x_{MW}(\vec{r})$, $\tilde{\mathcal{E}}_{(p1)}(\vec{k}_{p1})$ is the spatial Fourier transform of $\mathcal{E}_{(p1)}(\vec{r})$ (with other modes defined similarly), and $\tilde{\Gamma}(\vec{k})$ is the spatial Fourier transform of function $\Gamma(\vec{r})$. The extent to which the field modes are captured within $\Gamma(\vec{r})$ is also the extent to which its Fourier transform $\tilde{\Gamma}(\vec{k})$ may be approximated by a Dirac Delta function, enforcing momentum conservation. This is particularly important in evaluating transducer designs, where the sound propagates perpendicular to well-confined light—as in the transducer described in [5]—complicating analysis in terms of momentum conservation. In this case, the small transverse dimensions of the interacting medium facilitate coupling between large-enough transverse momenta to make transduction in this way possible. That said, the transduction efficiency (all other factors constant) would be lower than might otherwise be possible because the narrow uncertainty of the phonon momentum mode $\tilde{x}_{MW}(\vec{k})$ implies a broad-enough uncertainty in position that $x_{MW}(\vec{r})$ becomes heavily truncated by the dimensions of the interacting medium. While one can compensate for this with other factors, an optimal design obviates the challenges that come with doing so.

As a side benefit of optomechanical four-wave mixing, the conditions achieving the correct phase-matching in this process will generally not also satisfy the phase-matching conditions for optomechanical three-wave mixing. Because of this, the lower-order optomechanical coupling used in standard transducers will be suppressed at the same time that optomechanical four-wave mixing is optimized, removing it as a source of loss/noise.

IV. CONCLUSION

In this work, we have shown how the frequency filtering challenges in quantum transduction can be circumvented by utilizing optomechanical four-wave mixing. Moreover, we have given arguments for why this higher-order process ought to amount to comparable optomechanical coupling to the standard case. The benefits of this approach are not without their drawbacks, however. While optomechanical four-wave mixing has a power-scaling advantage in that its efficiency literally grows with pump power, its efficiency also varies with the phase of the pump, suggesting that additional stabilization may be required. Moreover, there will be additional optical design requirements for the transducer to be able to host a pair of wavelengths nearly an octave apart with maximal overlap/coupling. Independent of quantum transduction, this higher-order optomechanical connection may enable sensing technologies where using standard Brillouin scattering is impractical.

ACKNOWLEDGMENTS

We gratefully acknowledge support from our colleagues at the Air Force Research Laboratory (AFRL) and at Purdue University and, in particular, Dr. Samuel Schwab of AFRL, who inspired the refined analysis of momentum conservation seen in this work, as well as anonymous referees, whose detailed comments yielded substantial improvements and insights.

The views expressed are those of the authors and do not reflect the official guidance or position of the United States Government, the Department of Defense, or of the United States Air Force. The appearance of external hyperlinks does not constitute endorsement by the United States Department of Defense (DoD) of the linked websites, or of the information, products, or services contained therein. The DoD does not exercise any editorial, security, or other control over the information you may find at these locations.

APPENDIX A: THERMODYNAMIC RELATIONS BETWEEN ELECTRIC AND MECHANICAL DISPLACEMENT

Consider a dielectric solid at constant temperature T. With heat free to flow in/out of this system, and wanting temperature as an independent variable, we employ the Helmholtz free energy $A = U - TS$, instead of the internal energy U, to

describe the thermodynamics of this system. The differential change in its Helmholtz free energy A is given by

$$dA = -SdT + X_{ij}dx_{ij} + E_i dD_i, \tag{A1}$$

where S is the entropy, X_{ij} is the mechanical stress tensor, x_{ij} is the mechanical strain tensor, E_i is the ordinary electric field, and D_i is the electric displacement field. In addition, $-SdT$ is the differential heat flow into/out of the system; $X_{ij}dx_{ij}$ is the differential mechanical work done on/by the system; and $E_i dD_i$ is the differential electromagnetic work done on/by the system, where electromagnetic energy can be stored in a dielectric by induced polarization. Just as in the body of our work, we use the Einstein summation convention on repeated indices to condense notation, where, for example, $E_i dD_i$ is an inner product between the electric field, and the differential change in the electric displacement field.

With temperature T being constant, and because we can express A as a function of (T, x_{ij}, D_i), we may, in turn, express the mechanical stress tensor X_{ij} as a function of strain x_{ij}, and the electric displacement field D_i:

$$X_{ij} = \left(\frac{\partial A}{\partial x_{ij}}\right)_{(T,\bar{x},D)} = X_{ij}(x, D). \tag{A2}$$

Similarly, we may express the Electric field E_i as a function of these variables, as well:

$$E_i = \left(\frac{\partial A}{\partial D_i}\right)_{(T,\bar{x},D)} = E_i(x, D). \tag{A3}$$

Both X_{ij} and E_i can be Taylor-expanded in powers of x_{ij} and D_i. Since even relatively intense sound results in small displacements, we write out the Taylor expansion up to first-order in strain x_{ij} and up to third-order in the electric displacement field D_i (accounting for orders of strain):

$$X_{ij}(x,D) \approx \begin{bmatrix} \text{const} & + & \left(\frac{\partial X_{ij}}{\partial D_k}\Big|_{0,0} D_k & + & \frac{1}{2}\left(\frac{\partial^2 X_{ij}}{\partial D_k \partial D_\ell}\Big|_{0,0} D_k D_\ell & + & \frac{1}{3!}\left(\frac{\partial^3 X_{ij}}{\partial D_k \partial D_\ell \partial D_m}\Big|_{0,0} D_k D_\ell D_m \\ +\left(\frac{\partial X_{ij}}{\partial x_{k\ell}}\Big|_{0,0} x_{k\ell} & + & \frac{1}{2}\left(\frac{\partial^2 X_{ij}}{\partial x_{k\ell}\partial D_m}\Big|_{0,0} x_{k\ell} D_m & + & \frac{1}{3!}\left(\frac{\partial^3 X_{ij}}{\partial x_{k\ell}\partial D_m \partial D_n}\Big|_{0,0} x_{k\ell} D_m D_n & + & \cdots \end{bmatrix}, \tag{A4}$$

$$E_i(x,D) \approx \begin{bmatrix} \text{const} & + & \left(\frac{\partial E_i}{\partial D_k}\Big|_{0,0} D_k & + & \frac{1}{2}\left(\frac{\partial^2 E_i}{\partial D_k \partial D_\ell}\Big|_{0,0} D_k D_\ell & + & \frac{1}{3!}\left(\frac{\partial^3 E_i}{\partial D_k \partial D_\ell \partial D_m}\Big|_{0,0} D_k D_\ell D_m \\ +\left(\frac{\partial E_i}{\partial x_{k\ell}}\Big|_{0,0} x_{k\ell} & + & \frac{1}{2}\left(\frac{\partial^2 E_i}{\partial x_{k\ell}\partial D_m}\Big|_{0,0} x_{k\ell} D_m & + & \frac{1}{3!}\left(\frac{\partial^3 E_i}{\partial x_{k\ell}\partial D_m \partial D_n}\Big|_{0,0} x_{k\ell} D_m D_n & + & \cdots \end{bmatrix}. \tag{A5}$$

In terms of conventional tensors (where we truncate the power series so terms equivalent to second- and higher-order derivatives of the electric field, with respect to strain, are neglected), these expressions can be simplified as

$$X_{ij}(x,D) \approx \begin{bmatrix} \text{const} & + & (h_{ijk})D_k & + & \frac{1}{2}\left(\frac{p_{ijk\ell}}{\epsilon_0}\right)D_k D_\ell & + & \frac{1}{3!}\left(\frac{q_{ijk\ell m}}{\epsilon_0}\right)D_k D_\ell D_m \\ +(c_{ijk\ell})x_{k\ell} & + & \cdots \end{bmatrix}, \tag{A6}$$

$$E_i(x,D) \approx \begin{bmatrix} \text{const} & + & \eta^{(1)}_{ik} D_k & + & \eta^{(2)}_{ik\ell} D_k D_\ell & + & \eta^{(3)}_{ik\ell m} D_k D_\ell D_m \\ +(h_{k\ell i})x_{k\ell} & + & \frac{1}{2}\left(\frac{p_{mik\ell}}{\epsilon_0}\right)x_{k\ell} D_m & + & \frac{1}{3!}\left(\frac{2q_{k\ell mmi}}{\epsilon_0}\right)x_{k\ell} D_m D_n & + & \cdots \end{bmatrix}. \tag{A7}$$

Here, h_{ijk} is the stress-voltage form of the piezoelectric tensor [52], $p_{ijk\ell}$ is the photoelasticity tensor, and $q_{ijk\ell m}$ is what we are defining as the second-order photoelasticity, or cubic electrostriction, tensor.

The relations between different orders of electric and mechanical displacement are based on the equality of different orders of mixed partial derivatives of A (as define the Maxwell relations).

Where stress and the electric field are different first-derivatives of A, the first-order connection between mechanical stress and electric displacement is based on mixing second derivatives of A:

$$(h_{ijk}) \equiv \left(\frac{\partial X_{ij}}{\partial D_k}\right) \tag{A8a}$$

$$h_{ijk} = \left(\frac{\partial^2 A}{\partial D_k \partial x_{ij}}\right) = \left(\frac{\partial^2 A}{\partial x_{ij}\partial D_k}\right) = \left(\frac{\partial E_k}{\partial x_{ij}}\right). \tag{A8b}$$

Indeed, this relation defines the connection between forward and converse piezoelectricity.

Beyond simple piezoelectricity, we have that the second-order connection between mechanical stress and electric displacement is based on mixing third derivatives of A:

$$\left(\frac{\partial^2 X_{ij}}{\partial D_k \partial D_\ell}\right) = \left(\frac{\partial^3 A}{\partial D_k \partial D_\ell \partial x_{ij}}\right) = \left(\frac{\partial^3 A}{\partial x_{ij}\partial D_k \partial D_\ell}\right) = \left(\frac{\partial^2 E_\ell}{\partial x_{ij}\partial D_k}\right) = \left(\frac{\partial \eta_{\ell k}}{\partial x_{ij}}\right) \equiv \left(\frac{p_{k\ell ij}}{\epsilon_0}\right). \tag{A9}$$

Where $p_{ijk\ell}$ is the photoelasticity tensor, this second-order connection illustrates that it is related to a dependence of generated stress as a quadratic function of the electric field, i.e., electrostriction. This mechanism defines the conventional optomechanical coupling in transducers.

Beyond both piezoelectricity and standard electrostriction, we find third-order connection between mechanical stress and electric displacement based on mixing fourth derivatives of A:

$$\left(\frac{\partial^3 X_{ij}}{\partial D_k \partial D_\ell \partial D_m}\right) = \left(\frac{\partial^4 A}{\partial D_k \partial D_\ell D_m \partial x_{ij}}\right) = \left(\frac{\partial^4 A}{\partial x_{ij} \partial D_k \partial D_\ell \partial D_m}\right) = \left(\frac{\partial^3 E_m}{\partial x_{ij} \partial D_k \partial D_\ell}\right) = 2\left(\frac{\partial \eta^{(2)}_{m\ell k}}{\partial x_{ij}}\right) \equiv 2\frac{q_{ijk\ell m}}{\epsilon_0}. \tag{A10}$$

Note: The factor of two here comes from having to apply the product rule in the power series for $E_i = \eta_{ij} D_j$ [see Eq. (6) for η_{ij} series] when differentiating;

$$\frac{\partial^2 E_m}{\partial D_\ell \partial D_k} = \eta^{(2)}_{m\ell k} + \eta^{(2)}_{mk\ell}, \tag{A11}$$

and assuming $\eta^{(2)}_{m\ell k} = \eta^{(2)}_{mk\ell}$ (such as the case of Kleinman symmetry, where a lossless medium's nonlinear susceptibility is approximately independent of frequency [33]) and that the third-order susceptibility is negligible by comparison. This illustrates that the cubic electrostriction $q_{ijk\ell m}$ is up to a factor of two, equal to the second-order photoelasticity.

APPENDIX B: OPTOMECHANICAL COUPLING COMPARISON

In this Appendix, we rigorously demonstrate how one may determine a proper side-by-side comparison between the optomechanical coupling, utilizing ordinary photoelasticity, and our proposed mechanism, utilizing second-order photoelasticity.

The second-order photoelastic interaction Hamiltonian is given as

$$\hat{H}^{(2)}_{\text{int}} = \frac{1}{3\epsilon_0}\int d^3 r (q_{hijk\ell}\hat{D}_h\hat{D}_i\hat{D}_j\hat{x}_{k\ell}). \tag{B1}$$

If we sum over all $(6 = 3!)$ permutations of components of the product of electric displacement fields, we find

$$\hat{H}^{(2)}_{\text{int}} = \frac{2}{\epsilon_0}\int d^3 r (q_{(eff)k\ell}\hat{D}^{(+)}_{p0}\hat{D}^{(+)}_{p0}\hat{D}^{(-)}_{tr}\hat{x}^{(+)}_{k\ell}) + \text{H.c.}, \tag{B2}$$

where $\hat{D}_h = \hat{D}^{(+)}_h + \hat{D}^{(-)}_h$ and we neglect non-energy-conserving terms in the interaction. In general, this interaction occurs only in the region of space where $q_{(\text{eff})k\ell}$ is significant, limiting us to integrate over the dimensions of the nonlinear medium. This effect can be included by replacing $q_{(\text{eff})k\ell}$ with $q_{(\text{eff})k\ell}\Gamma(\vec{r})$ inside the integral, where $\Gamma(\vec{r})$ is a bounding function that is unity within the interacting medium, and zero outside the interacting medium. We leave the analysis of $\Gamma(\vec{r})$ and its effects to the next Appendix. This Hamiltonian reflects events where two pump photons and a phonon are annihilated to create a transduced photon and vise versa. In this case, the quantum operators for these fields are given by

$$\hat{D}^{(+)}_j(\vec{r},t) = i\sum_m \sqrt{\frac{\hbar\omega_m}{2\eta_{\text{eff},(m)}V^{EM(m)}_{\text{eff}}}}\mathcal{E}_{(j,m)}(\vec{r})\hat{a}_{(j,m)}(t), \tag{B3}$$

and

$$\hat{x}^{(+)}_{k\ell}(\vec{r},t) = \frac{\partial \hat{u}^{(+)}_k(\vec{r},t)}{\partial r_\ell} = \sum_q \sqrt{\frac{\hbar}{2m^{(q)}_{\text{eff}}\omega_q}}\frac{\partial w_{(k,q)}(\vec{r})}{\partial r_\ell}\hat{b}_q(t), \tag{B4}$$

with mode functions $\mathcal{E}_{(j,m)}(\vec{r})$ and $w_{(k,q)}(\vec{r})$ normalized by

$$\int d^3 r \sum_{ij}\eta_{ij}(\vec{r})\mathcal{E}_{(j,m)}(\vec{r})\mathcal{E}^*_{(i,m')}(\vec{r}) = \delta_{mm'}\eta_{\text{eff},(m)}V^{EM(m)}_{\text{eff}}, \tag{B5a}$$

$$\int d^3 r \sum_i |w_{(i,q)}(\vec{r})|^2 = V^{\text{mech}(q)}_{\text{eff}}, \tag{B5b}$$

and where the electromagnetic and acoustic mode volumes are defined similarly to one another:

$$V^{EM(m)}_{\text{eff}} = \frac{\left(\int d^3 r \sum_{ij}\eta_{ij}(\vec{r})\mathcal{E}_{(j,m)}(\vec{r})\mathcal{E}^*_{(i,m)}(\vec{r})\right)^2}{\int d^3 r\left(\sum_{ij}\eta_{ij}(\vec{r})\mathcal{E}_{(j,m)}(\vec{r})\mathcal{E}^*_{(i,m)}(\vec{r})\right)^2}, \tag{B6a}$$

$$V^{\text{mech}(q)}_{\text{eff}} = \left(\int d^3 r\left(\frac{\sum_i |w_{(i,q)}(\vec{r})|^2}{\int d^3 r' \sum_i |w_{(i,q)}(\vec{r}')|^2}\right)^2\right)^{-1}. \tag{B6b}$$

Note: In the body of this work, we replace the expression $\frac{\partial w_{(k,q)}(\vec{r})}{\partial r_\ell}$ with the expression $x_{\text{mech}}(\vec{r})$ to condense notation.

If we consider only a single mode from each field participating in the interaction, and note that $\rho_{\text{eff}}V^{(q)}_{\text{eff}} = m^{(q)}_{\text{eff}}$, the interaction Hamiltonian has the following relatively simple form:

$$\hat{H}^{(2)}_{\text{int}} = iq_{(\text{eff})k\ell}\sqrt{\frac{\hbar^4\omega_{p1}\omega_{p2}\omega_{tr}}{4\epsilon_0^2\eta_{p1}\eta_{p2}\eta_{tr}\rho_{\text{eff}}\omega_{MW}\left(V^{EM}_{\text{eff}}\right)^3 V^{(\text{mech})}_{\text{eff}}}}\left(\int d^3 r\mathcal{E}_{(p1)}(\vec{r})\mathcal{E}_{(p2)}(\vec{r})\mathcal{E}^*_{(tr)}(\vec{r})\frac{\partial w_{(k,MW)}(\vec{r})}{\partial r_\ell}\right) \times \hat{a}_{p1}(t)\hat{a}_{p2}(t)\hat{a}^\dagger_{tr}(t)\hat{b}_{MW}(t) + \text{H.c.}. \tag{B7}$$

For the first-order photoelastic interaction, we have

$$\hat{H}^{(1)}_{\text{int}} = \frac{1}{2\epsilon_0}\int d^3 r\left(p^{(\text{eff})}_{ijk\ell}\hat{D}_i\hat{D}_j\hat{x}_{k\ell}\right). \tag{B8}$$

If we sum over both permutations of components of the product of electric displacement fields, we find:

$$\hat{H}^{(1)}_{\text{int}} = \frac{1}{\epsilon_0}\int d^3r\left(p_{(\text{eff})k\ell}\hat{D}^{(+)}_{p}\hat{D}^{(-)}_{tr}\hat{x}^{(+)}_{k\ell}\right) + \text{H.c.}. \tag{B9}$$

In the single-mode approximation, this Hamiltonian has the following form:

$$\hat{H}^{(1)}_{\text{int}} = p_{(\text{eff})k\ell}\sqrt{\frac{\hbar^3\omega_p\omega_{tr}}{8\epsilon_0^2\eta_p\eta_{tr}\rho_{\text{eff}}\omega_{MW}\left(V^{EM}_{\text{eff}}\right)^2 V^{(\text{mech})}_{\text{eff}}}}\left(\int d^3r\mathcal{E}_{(p)}(\vec{r})\mathcal{E}^*_{(tr)}(\vec{r})\frac{\partial w_{(k,MW)}(\vec{r})}{\partial r_\ell}\right)\hat{a}_p(t)\hat{a}^\dagger_{tr}(t)\hat{b}_{MW}(t) + \text{H.c.}. \tag{B10}$$

To properly isolate when these interactions will be of equal strength, we must see when

$$\left|\frac{\alpha_p p_{(\text{eff})k\ell}\sqrt{\frac{\hbar^3\omega_p\omega_t}{8\rho_{(\text{eff})}\epsilon_0^2\eta_p\eta_t V^{\text{mech}}_{\text{eff}}\left(V^{EM}_{\text{eff}}\right)^2\omega_{MW}}}}{\alpha^2_{p0}q_{(\text{eff})k\ell}\sqrt{\frac{\hbar^4\omega^2_{p0}\omega_t}{4\rho_{(\text{eff})}\epsilon_0^2\eta^2_{p0}\eta_t V^{\text{mech}}_{\text{eff}}\left(V^{EM}_{\text{eff}}\right)^3\omega_{MW}}}}\frac{\left(\int d^3r\mathcal{E}_{(p)}(\vec{r})\mathcal{E}^*_{(tr)}(\vec{r})\frac{\partial w_{(k,MW)}(\vec{r})}{\partial r_\ell}\right)}{\left(\int d^3r\mathcal{E}_{(p1)}(\vec{r})\mathcal{E}_{(p2)}(\vec{r})\mathcal{E}^*_{(tr)}(\vec{r})\frac{\partial w_{(k,MW)}(\vec{r})}{\partial r_\ell}\right)}\right| \approx 1. \tag{B11}$$

Here, we have replaced pump fields with their coherent state amplitudes (implicitly assuming an undepleted pump approximation). Among other aspects, we have from the orthogonality relation between electromagnetic modes that inside the spatial-overlap integral,

$$\mathcal{E}_{p1}(\vec{r}) \sim \sqrt{V^{EM}_{\text{eff}}}, \tag{B12}$$

which yields the following substantially simplified comparison:

$$\frac{p_{(\text{eff})k\ell}\alpha_p}{q_{(\text{eff})k\ell}\alpha^2_{p0}}\sqrt{\frac{\omega_p\eta^2_{p0}}{2\hbar\omega^2_{p0}\eta_p}} \approx 1. \tag{B13}$$

Assuming that the susceptibility is approximately independent of frequency over the bands of interest, we can simplify things further. If we substitute the coherent state amplitudes for their corresponding expressions of photon number or energy, i.e., $\alpha_{p0} = \sqrt{N_{p0}} = \sqrt{U_{p0}/(\hbar\omega_{p0})}$:

$$|p_{(\text{eff})k\ell}| \approx \left|q_{(\text{eff})k\ell}\sqrt{\frac{2U_{p0}}{\eta_{p0}}}\right|. \tag{B14}$$

Recalling that our virtual photoelasticity was given as

$$p^{(\text{virt})}_{(\text{eff})k\ell} = 2q_{(\text{eff})k\ell}D_{p0}, \tag{B15}$$

we can verify its approximation by examining the expression for the pump energy U_{p0}, which results by equating these two expressions for the photoelasticity:

$$U_{p0} = 2\eta_{p0}D^2_{p0} = 2D_{p0}E_{p0}. \tag{B16}$$

This relation is consistent with the energy-density of the electromagnetic field when we recall that the energy is evenly split between electric and magnetic components, as well as between positive and negative frequency components.

APPENDIX C: PHASE MATCHING AND MOMENTUM CONSERVATION IN THE OVERLAP INTEGRAL

Given N interacting bosonic modes described by mode functions $g_s(\vec{r})$, where s ranges from 1 to N, and a bounding function $\Gamma(\vec{r})$ that is unity inside the interaction region and zero outside the interaction region, the overlap integral Φ_N is defined as

$$\Phi_N = \int d^3r\ \Gamma(\vec{r})g_1(\vec{r})g_2(\vec{r})g_3(\vec{r})...g_N(\vec{r}). \tag{C1}$$

Taking $\tilde{g}_s(\vec{k}_s)$ to be the spatial Fourier transform of $g_s(\vec{r})$, this overlap integral can be expressed in momentum space:

$$\Phi_N = \int d^3r\left(\frac{1}{(2\pi)^{3/2}}\int d^3k_0\tilde{\Gamma}(\vec{k}_0)e^{i\vec{k}_0\cdot\vec{r}}\right)\prod_{s=1}^{N}\left(\frac{1}{(2\pi)^{3/2}}\int d^3k_s\tilde{g}_s(\vec{k}_s)e^{i\vec{k}_s\cdot\vec{r}}\right), \tag{C2a}$$

$$= \left(\frac{1}{(2\pi)^{3(N+1)/2}}\right)\int d^3r\left(\int d^3k_0\int d^3k_1\int d^3k_2\int ...\int d^3k_N\tilde{\Gamma}(\vec{k}_0)(\tilde{g}_1(\vec{k}_1)\tilde{g}_2(\vec{k}_2)...\tilde{g}_N(\vec{k}_N))e^{i(\vec{k}_0+\vec{k}_1+\vec{k}_2+...+\vec{k}_N)\cdot\vec{r}}\right), \tag{C2b}$$

$$= \left(\frac{1}{(2\pi)^{3(N+1)/2}}\right)\left(\int d^3k_0\int d^3k_1\int d^3k_2\int ...\int d^3k_N\tilde{\Gamma}(\vec{k}_0)(\tilde{g}_1(\vec{k}_1)\tilde{g}_2(\vec{k}_2)...\tilde{g}_N(\vec{k}_N))\int d^3re^{i(\vec{k}_0+\vec{k}_1+\vec{k}_2+...+\vec{k}_N)\cdot\vec{r}}\right), \tag{C2c}$$

$$= \left(\frac{(2\pi)^{3N}}{(2\pi)^{3(N+1)/2}}\right)\left(\int d^3k_0\int d^3k_1\int d^3k_2\int ...\int d^3k_N\tilde{\Gamma}(\vec{k}_0)(\tilde{g}_1(\vec{k}_1)\tilde{g}_2(\vec{k}_2)...\tilde{g}_N(\vec{k}_N))\delta(\vec{k}_0+\vec{k}_1+\vec{k}_2+...+\vec{k}_N)\right), \tag{C2d}$$

$$= (2\pi)^{3(N-1)/2}\left(\int d^3k_1\int d^3k_2\int ...\int d^3k_N\right)(\tilde{g}_1(\vec{k}_1)\tilde{g}_2(\vec{k}_2)...\tilde{g}_N(\vec{k}_N))\tilde{\Gamma}(\vec{k}_1+\vec{k}_2+...+\vec{k}_N). \tag{C2e}$$

Here, we have: expressed each mode function and the bounding function in terms of its respective Fourier transforms; consolidated the product of integrals as a joint integral over a product of functions; grouped the exponentials together and integrated over all components of position $\vec{r}$ to obtain a Dirac Delta function; and integrated over all components of the bounding-function momentum $\vec{k}_0$ to eliminate the Dirac Delta function, leading to our final result. The extent to which the bounding function $\Gamma(\vec{r})$ completely encapsulates the mode functions in position space is the extent to which its transform $\tilde{\Gamma}(\vec{k})$ may be treated as a Dirac Delta function in the overlap integral, defining the degree of momentum-conservation enforcement.

Note that this overlap integral is well-defined whether or not the domains of the mode functions allow for momentum conservation. In the event that they do not, such as when $\tilde{g}(\vec{k}_1)$ has a range that's offset from its otherwise-optimum value, this offset will manifest as a rapidly oscillating phase in the conjugate (spatial) domain over which the overlap integral washes out to zero.

Moreover, when the spatial modes can approximately be expressed as a product of a transverse mode function (of transverse coordinates) and a longitudinal mode function (of longitudinal coordinate), this analysis of the overlap integral factors approximately into that of a transverse overlap integral times the longitudinal overlap integral (often regarded as the phase-matching integral for beamlike modes). In this case of beamlike propagation, the conservation of transverse momentum implies the conservation of the longitudinal component of angular momentum, i.e., orbital angular momentum (OAM) about the propagation axis, whose eigenfunctions are OAM modes.

[1] N. Lauk, N. Sinclair, S. Barzanjeh, J. P. Covey, M. Saffman, M. Spiropulu, and C. Simon, Perspectives on quantum transduction, Quantum Sci. Technol. **5**, 020501 (2020).

[2] X. Han, W. Fu, C.-L. Zou, L. Jiang, and H. X. Tang, Microwave-optical quantum frequency conversion, Optica **8**, 1050 (2021).

[3] D. Awschalom, K. K. Berggren, H. Bernien, S. Bhave, L. D. Carr, P. Davids, S. E. Economou, D. Englund, A. Faraon, M. Fejer *et al.*, Development of quantum interconnects (QuICs) for next-generation information technologies, PRX Quantum **2**, 017002 (2021).

[4] X. Xu, Y. Zhang, J. Tang, P. Chen, L. Zeng, Z. Xia, W. Xing, Q. Zhou, Y. Wang, H. Song *et al.*, Optomechanical microwave-to-optical photon transducer chips: Empowering the quantum internet revolution, Micromachines **15**, 485 (2024).

[5] T. Blésin, H. Tian, S. A. Bhave, and T. J. Kippenberg, Quantum coherent microwave-optical transduction using high-overtone bulk acoustic resonances, Phys. Rev. A **104**, 052601 (2021).

[6] M. J. Weaver, P. Duivestein, A. C. Bernasconi, S. Scharmer, M. Lemang, T. C. v. Thiel, F. Hijazi, B. Hensen, S. Gröblacher, and R. Stockill, An integrated microwave-to-optics interface for scalable quantum computing, Nat. Nanotechnol. **19**, 166 (2024).

[7] M. Mirhosseini, A. Sipahigil, M. Kalaee, and O. Painter, Superconducting qubit to optical photon transduction, Nature (London) **588**, 599 (2020).

[8] X. Han, W. Fu, C. Zhong, C.-L. Zou, Y. Xu, A. A. Sayem, M. Xu, S. Wang, R. Cheng, L. Jiang *et al.*, Cavity piezo-mechanics for superconducting-nanophotonic quantum interface, Nat. Commun. **11**, 3237 (2020).

[9] T. Blésin, W. Kao, A. Siddharth, R. N. Wang, A. Attanasio, H. Tian, S. A. Bhave, and T. J. Kippenberg, Bidirectional microwave-optical transduction based on integration of high-overtone bulk acoustic resonators and photonic circuits, Nat. Commun. **15**, 6096 (2024).

[10] D. J. Starling, S. M. Bloch, P. K. Vudyasetu, J. S. Choi, B. Little, and J. C. Howell, Double Lorentzian atomic prism, Phys. Rev. A **86**, 023826 (2012).

[11] M. Shirasaki, Virtually imaged phased array as a wavelength demultiplexer, U.S. Patent 5 999 320 (Dec. 7, 1999).

[12] S. Xiao, A. M. Weiner, and C. Lin, A dispersion law for virtually imaged phased-array spectral dispersers based on paraxial wave theory, IEEE J. Quantum Electron. **40**, 420 (2004).

[13] S. Krastanov, H. Raniwala, J. Holzgrafe, K. Jacobs, M. Lončar, M. J. Reagor, and D. R. Englund, Optically heralded entanglement of superconducting systems in quantum networks, Phys. Rev. Lett. **127**, 040503 (2021).

[14] S. Meesala, S. Wood, D. Lake, P. Chiappina, C. Zhong, A. D. Beyer, M. D. Shaw, L. Jiang, and O. Painter, Non-classical microwave–optical photon pair generation with a chip-scale transducer, Nat. Phys. **20**, 871 (2024).

[15] S. Meesala, D. Lake, S. Wood, P. Chiappina, C. Zhong, A. D. Beyer, M. D. Shaw, L. Jiang, and O. Painter, Quantum entanglement between optical and microwave photonic qubits, Phys. Rev. X **14**, 031055 (2024).

[16] W. Jiang, F. M. Mayor, S. Malik, R. Van Laer, T. P. McKenna, R. N. Patel, J. D. Witmer, and A. H. Safavi-Naeini, Optically heralded microwave photon addition, Nat. Phys. **19**, 1423 (2023).

[17] N. Fiaschi, B. Hensen, A. Wallucks, R. Benevides, J. Li, T. P. M. Alegre, and S. Gröblacher, Optomechanical quantum teleportation, Nat. Photon. **15**, 817 (2021).

[18] D. Voss, M. Lucibella, K. Johnson, and N. Bennett-Karasik, March 1880: The curie brothers discover piezoelectricity, American Physical Society (2014).

[19] H. Osterberg and J. W. Cookson, The piezodielectric effect and electrostriction in anisotropic or isotropic media, Phys. Rev. **51**, 1096 (1937).

[20] F. Barocchi, Multiphoton-phonon interactions and higher order Brillouin scattering: (steady-state gain amplification), Opt. Commun. **3**, 189 (1971).

[21] A. N. Cleland, *Foundations of Nanomechanics: From Solid-State Theory to Device Applications* (Springer Science & Business Media, New York, 2013).

[22] J.-W. Jeong, S.-C. Shin, I. L. Lyubchanskii, and V. N. Varyukhin, Strain-induced three-photon effects, Phys. Rev. B **62**, 13455 (2000).

[23] A. Zibrov, A. Matsko, and M. Scully, Four-wave mixing of optical and microwave fields, Phys. Rev. Lett. **89**, 103601 (2002).

[24] J. P. Covey, A. Sipahigil, and M. Saffman, Microwave-to-optical conversion via four-wave mixing in a cold ytterbium ensemble, Phys. Rev. A **100**, 012307 (2019).

[25] S. Borówka, U. Pylypenko, M. Mazelanik, and M. Parniak, Continuous wideband microwave-to-optical converter based on room-temperature Rydberg atoms, Nat. Photon. **18**, 32 (2024).

[26] A. Kumar, A. Suleymanzade, M. Stone, L. Taneja, A. Anferov, D. I. Schuster, and J. Simon, Quantum-enabled millimetre wave to optical transduction using neutral atoms, Nature (London) **615**, 614 (2023).

[27] J. Schneeloch, E. Sheridan, A. M. Smith, C. C. Tison, D. L. Campbell, M. D. LaHaye, M. L. Fanto, and P. M. Alsing, Principles for optimizing quantum transduction in piezo-optomechanical systems, Phys. Rev. A **111**, 052605 (2025).

[28] B. E. Saleh and M. C. Teich, *Fundamentals of Photonics Part II: Photonics*, 3rd ed. (John Wiley & Sons, Inc., Hoboken, New Jersey, 2019), Chap. 20.3, pp. 967–971.

[29] N. Quesada and J. Sipe, Why you should not use the electric field to quantize in nonlinear optics, Opt. Lett. **42**, 3443 (2017).

[30] J. Schneeloch, S. H. Knarr, D. F. Bogorin, M. L. Levangie, C. C. Tison, R. Frank, G. A. Howland, M. L. Fanto, and P. M. Alsing, Introduction to the absolute brightness and number statistics in spontaneous parametric down-conversion, J. Opt. **21**, 043501 (2019).

[31] The different factor of $1/3$ for $\hat{H}^{(2)}_{\rm int}$ vs $\hat{H}^{(1)}_{\rm int}$ is a consequence of there being three interacting displacement fields in this portion of the total field energy. For a fuller discussion, see [29,30].

[32] R. C. Miller, Optical second harmonic generation in piezoelectric crystals, Appl. Phys. Lett. **5**, 17 (1964).

[33] R. W. Boyd, *Nonlinear Optics*, 3rd ed. (Academic Press, Burlington, Massachusetts, 2008).

[34] When accounting for quasi-phase-matching, where the medium is periodically poled to periodically flip the sign of the second-order nonlinear optical susceptibility over the length of the medium, $d_{\rm eff}$ decreases from its nominal value by a factor of $2/(n\pi)$, where n is the diffraction order (ideally unity).

[35] E. Palik, *Handbook of Optical Constants of Solids, Five-Volume Set: Handbook of Thermo-Optic Coefficients of Optical Materials with Applications* (Elsevier Science, San Diego, California, 1997).

[36] J. Zhou, M. Liu, C. Zhou, B. H. Kuo, F.-S. Shieu, and P. T. Lin, Mid-infrared nonlinear frequency conversion using monolithic barium titanate on silicon-on-insulator, IEEE J. Sel. Top. Quantum Electron. **29**, 1 (2023).

[37] * This is an order-of-magnitude estimate based on SHG from 3.1–1.55 microns in [36].

[38] Note: The electro-optic (Pockels) tensor and the $\chi^{(2)}$ nonlinear susceptibility tensor describe the same nonlinear response, albeit in very different frequency bands. The Pockels tensor is tabulated at low (DC-GHz) frequencies, while the nonlinear susceptibility is defined at much higher (optical) frequencies. The exceptionally large (of order 10^3pm/V) electro-optic coefficient of barium titanate does not immediately imply a correspondingly large value for $d_{\rm eff}$.

[39] M. Zgonik, P. Bernasconi, M. Duelli, R. Schlesser, P. Günter, M. H. Garrett, D. Rytz, Y. Zhu, and X. Wu, Dielectric, elastic, piezoelectric, electro-optic, and elasto-optic tensors of $BaTiO_3$ crystals, Phys. Rev. B **50**, 5941 (1994).

[40] ** This is an order-of-magnitude estimate based on photoelasticity at 633 nm obtained from [39].

[41] D. E. Zelmon, D. L. Small, and D. Jundt, Infrared corrected sellmeier coefficients for congruently grown lithium niobate and 5 mol.% magnesium oxide–doped lithium niobate, J. Opt. Soc. Am. B **14**, 3319 (1997).

[42] B. Mytsyk, N. Demyanyshyn, A. Andrushchak, and O. Buryy, Photoelastic properties of trigonal crystals, Crystals **11**, 1095 (2021).

[43] *CRC Handbook of Chemistry and Physics*, 96th ed., edited by W. M. Haynes (CRC press, Boca Raton, Florida, 2015).

[44] R. S. Jacobsen, K. N. Andersen, P. I. Borel, J. Fage-Pedersen, L. H. Frandsen, O. Hansen, M. Kristensen, A. V. Lavrinenko, G. Moulin, H. Ou *et al.*, Strained silicon as a new electro-optic material, Nature (London) **441**, 199 (2006).

[45] J. B. Khurgin, T. H. Stievater, M. W. Pruessner, and W. S. Rabinovich, On the origin of the second-order nonlinearity in strained Si–SiN structures, J. Opt. Soc. Am. B **32**, 2494 (2015).

[46] M. Borghi, M. Mancinelli, F. Merget, J. Witzens, M. Bernard, M. Ghulinyan, G. Pucker, and L. Pavesi, High-frequency electro-optic measurement of strained silicon racetrack resonators, Opt. Lett. **40**, 5287 (2015).

[47] The mode field diameter chosen here is an order-of-magnitude estimate from step-index single-mode fiber optics assuming a Barium titanate core embedded in a silica cladding, where the core radius is chosen to minimize the MFD, subject to a constant wavelength.

[48] P. Mathey, S. Latour, P. Lompré, P. Jullien, D. Rytz, and B. Salce, Temperature distribution and thermal-induced defects in photorefractive barium titanate crystals illuminated with intense cw or pulsed laser irradiations, Appl. Phys. B **71**, 523 (2000).

[49] For comparison, the breakdown field in air is only about 3×10^6 V/m [43].

[50] P. Chiappina, J. Banker, S. Meesala, D. Lake, S. Wood, and O. Painter, Design of an ultra-low mode volume piezo-optomechanical quantum transducer, Opt. Express **31**, 22914 (2023).

[51] R. W. Terhune, P. D. Maker, and C. M. Savage, Optical harmonic generation in calcite, Phys. Rev. Lett. **8**, 404 (1962).

[52] Note that the more common stress-charge form of the piezoelectric tensor is e_{ijk}, such that $h_{ijk} = \eta_{im} e_{mjk}$.